



OPEN

SUBJECT AREAS:

INFLAMMATION
CELL SIGNALLING

Received

19 May 2014

Accepted

18 August 2014

Published

9 September 2014

Correspondence and requests for materials should be addressed to B.F.G. (B.F.Gibbs@kent.ac.uk) or V.V.S. (V.Sumbayev@kent.ac.uk)

Crucial involvement of xanthine oxidase in the intracellular signalling networks associated with human myeloid cell function

Maryam Abooli, Gurprit S. Lall, Karen Coughlan, Harjinder S. Lall, Bernhard F. Gibbs & Vadim V. Sumbayev

School of Pharmacy, University of Kent, Chatham Maritime, ME4 4TB, United Kingdom.

Xanthine oxidase (XOD) is an enzyme which plays a central role in purine catabolism by converting hypoxanthine into xanthine and then further into uric acid. Here we report that XOD is activated in THP-1 human myeloid cells in response to pro-inflammatory and growth factor stimulation. This effect occurred following stimulation of THP-1 cells with ligands of plasma membrane associated TLRs 2 and 4, endosomal TLRs 7 and 8 as well as stem cell growth factor (SCF). Hypoxia-inducible factor 1 (HIF-1) and activator protein 1 (AP-1) transcription complexes were found to be responsible for XOD upregulation. Importantly, the mammalian target of rapamycin (mTOR), a major myeloid cell translation regulator, was also found to be essential for XOD activation. Specific inhibition of XOD by allopurinol and sodium tungstate led to an increase in intracellular AMP levels triggering downregulation of mTOR activation by phosphorylation of its T2446 residue. Taken together, our results demonstrate for the first time that XOD is not only activated by pro-inflammatory stimuli or SCF but also plays an important role in maintaining mTOR-dependent translational control during the biological responses of human myeloid cells.

Xanthine oxidase (XOD), also known as xanthine oxidoreductase, is the enzyme which plays a central role in purine catabolism by utilising biologically active nucleotides arising from the degradation of nucleic acids and nucleotide mediators¹. XOD has two inter-convertible isoforms – oxygen-dependent oxidase and NAD⁺-dependent dehydrogenase. Both isoforms catalyse the conversion of hypoxanthine into xanthine and then further into uric acid (UA), the two terminal reactions of purine degradation pathway in humans, primates and birds. XOD is a homodimer (reported molecular weight – 283–290 KD) composed of two catalytically independent subunits with an approximate molecular weight of 150–155 KD^{1,2}. Each monomer contains 3 subunits with a mass of either 20, 40 or 85 KD, which can be separated from each other only under strong denaturing conditions. Each monomer contains 2 iron-sulphur clusters (Fe₂-S₂, located in the 20 KD subunit), 1 flavin adenine dinucleotide molecule (FAD, located in the 40 KD subunit) and the molybdenum (Mo) cofactor which is bound to the enzyme as molybdopterin (located in the 85 KD subunit). Each full-length (150 KD) monomer displays catalytic activity but neither of the smaller fragments can catalyse the XOD reaction since all the cofactors are required for the catalytic act^{1,2}.

For almost 100 years XOD was known as a purine catabolising enzyme that generates UA, a poorly soluble compound which may become accumulated in the synovial tissue³. While XOD was also recognised as a superoxide producer it was not considered as a main contributor to the cellular reactive oxygen species (ROS) pool⁴, except the cases of reperfusion injury. Recently, increasing evidence suggests that XOD plays a role in the biochemical regulation of myeloid cell function thus promoting their inflammatory state⁵. However, basic biochemical mechanisms underlying the functional role of this enzyme in maintaining the functional control of myeloid cell biological activity have not been elucidated. It was found that inflammatory stimuli like lipopolysaccharide (LPS, toll-like receptor (TLR) 4 ligand), resiquimod (R848, endosomal TLR7/8 ligand), and cytokines – tumour necrosis factor alpha, interleukin 1 beta (IL-1 β), interleukin 6 (IL-6) and interferon γ ^{1,6,7} induce XOD activation. Our recent findings demonstrated that XOD activity in myeloid cells is required for TLR/ligand-associated activation of the inflammasome, a multiprotein complex which catalyzes proteolytic reactions leading to the maturation of highly inflammatory cytokines belonging to the IL-1 β family⁶.



XOD activity has also been found to be increased under hypoxic conditions, which often form a physiological environment for myeloid cell responses. We also found that the pro-inflammatory upregulation of XOD activity in myeloid cells requires activation of the hypoxia-inducible factor 1 (HIF-1) transcription complex, which controls the adaptation of myeloid cells to signalling stress^{8–10}. The XOD gene promoter region (this gene contains >60 kb with 36 exons and is located in the short arm of human chromosome 2)^{11,12} contains two hypoxia-responsive elements (HIF-1 responsive) and 5 elements responsive to the activator protein 1 (AP1) transcription complex. Interestingly, a ligand/receptor-specific cross-link between the activities of XOD and HIF-1 has also been demonstrated⁶. Furthermore, XOD inhibitors were found to downregulate S2448 phosphorylation of the mammalian target of rapamycin (mTOR), which is required for activation of this kinase and plays a major role in the translational control of cellular responses and is essential for myeloid cell function¹³. Downstream responses of mTOR in myeloid cells could also be downregulated by XOD inhibitors in myeloid leukaemia cells^{7,10}.

Despite the above, there is, however, currently no clear evidence regarding the mechanisms of XOD activation in myeloid cells at either a transcriptional, translational or post-translational stage. All three mechanisms or their combination appear possible in the case of an enzyme such as XOD. Despite the evidence described, a conceptual basic knowledge of the mechanisms of XOD activation and its functional role is still almost absent. Here, we report that XOD is indeed activated in human myeloid leukaemia cells in response to pro-inflammatory and growth factor stimulation. This effect was observed when treating the cells with ligands of plasma membrane associated TLRs 2 and 4, endosomal TLRs 7 and 8 as well as stem cell factor (SCF). HIF-1 and activator protein 1 (AP-1) transcription factors were found to be responsible for XOD upregulation. Importantly, mTOR, a major myeloid cell translation regulator was found to be crucial for XOD activation as well. p38 MAP kinase appeared critical for XOD activation during the biological responses of human myeloid leukaemia cells triggered through plasma membrane-associated - but not endosomal - TLRs. Specific inhibition of XOD by allopurinol and sodium tungstate led to an increase in intracellular AMP levels triggering the downregulation of mTOR activation by phosphorylation of its T2446 residue. Our results suggest that XOD is important for maintaining intracellular AMP levels during the biological responses of human myeloid leukaemia cells. This is critical for activation of the mTOR pathway required for the biological responses of human myeloid cells. XOD appears, therefore, to be both an upstream regulator as well as a downstream target of the mTOR pathway.

Results

TLR ligands and SCF induce XOD activation, production of UA and S2448 mTOR phosphorylation. THP-1 human myeloid leukaemia cells expressing TLRs 2, 4, 7 and 8 as well as the pro-leukaemic SCF/Kit receptor^{7,8,10,14} were used for the experiments. Relative XOD expression was assessed by Western blotting (a full membrane is presented in Supplementary Figure 1) and the relative activity of the enzyme was analysed as outlined in the Materials and Methods. We observed that monocytic THP-1 cells expressed detectable amounts of XOD which were increased upon PMA-induced differentiation (24 h of exposure to 100 nM PMA, Figure 1). LAD2 mast cells expressed higher levels of XOD as did MCF-7 epithelial human breast cancer cells (Figure 1). Mouse liver homogenates were used as a positive control, since cells of this organ are known to express the highest levels of XOD¹⁵. The obtained results were consistent with those reported in the literature^{5,15}. Since monocytes are majorly involved in innate immune responses and remain SCF-dependent upon malignant transformation, we used non-differentiated THP-1 cells for further experiments⁷.

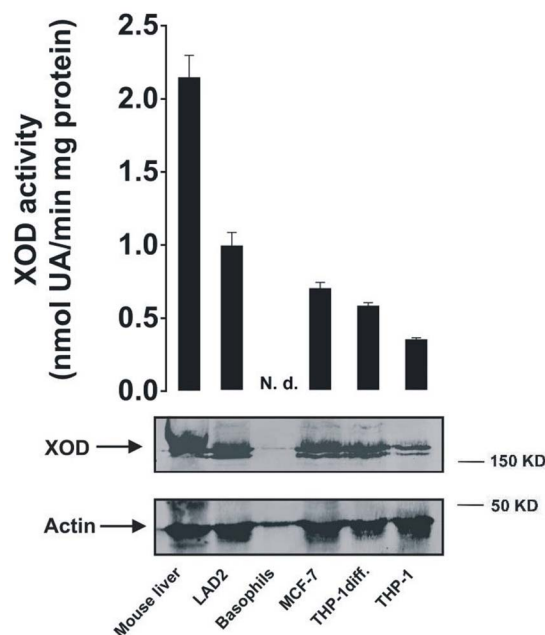


Figure 1 | XOD expression levels and relative activity in different cell types. XOD protein levels were detected in non-differentiated THP-1 cells, differentiated THP-1 cells (following 2h exposure to 100 nM PMA), primary human basophils, LAD2 mast cells and mouse liver homogenates. Relative XOD activity was also measured as outlined in Materials and Methods. Western blot data show one representative experiment of three that produced similar results and were quantitatively analysed. Cropped blots are used. Full-length blots are presented in Supplementary Figure 1. Other quantitative data are shown as mean values \pm S.D. of at least three independent experiments ($n=3$).

We exposed THP-1 cells to 1 μ g/ml lipopolysaccharide (LPS, TLR4 ligand), 1 μ g/ml peptidoglycan (PGN, TLR2 ligand), 0.1 μ g/ml R848 (TLR7/8 ligand) as well as 0.1 μ g/ml SCF for different periods of time. XOD activity was assessed using two methods (one based on the UA detection and another one based on the measurement of XOD-produced hydrogen peroxide, see Materials and Methods). We also analysed intracellular UA concentrations and phospho-S2448 mTOR. We found that XOD activity and UA levels were significantly increased by all the stimuli used. This was in line with a significant increase in mTOR S2448 phosphorylation (Figure 2).

Ligand-induced TLR2, 4, 7/8 and Kit-mediated XOD activation depends on HIF-1 and AP-1 transcription complexes and mTOR.

To assess the role of the HIF-1 transcription complex in XOD activation we used normal and HIF-1 α knockdown THP-1 cells (the alpha subunit of HIF-1 is an inducible one which acts as a limiting factor of HIF-1 activity)¹⁶. Cells were exposed to 1 μ g/ml LPS, 1 μ g/ml PGN, 0.1 μ g/ml R848 as well as 0.1 μ g/ml SCF for 4 h followed by detection of intracellular XOD protein levels and catalytic activity (Figure 3A). We found that treatment of the cells with all the above stimuli did not significantly upregulate XOD protein levels but significantly increased its activity. HIF-1 α knockdown THP-1 cells expressed lower levels of XOD and its activity was significantly affected (Figure 3A). Successful HIF-1 α silencing was controlled by qRT-PCR (see Supplementary Figure 4).

Pre-treatment of THP-1 cells for 1 h with 1 μ M AP-1 inhibitor SR 11302 (Tocris) followed by 4 h of treatments with LPS, PGN, R848 and SCF, as shown in Figure 3B, significantly reduced XOD expression and, as a result, dramatically reduced its catalytic activity (Figure 3B). The observed downregulatory effect was stronger compared to HIF-1 α knockdown, which confirms previous findings

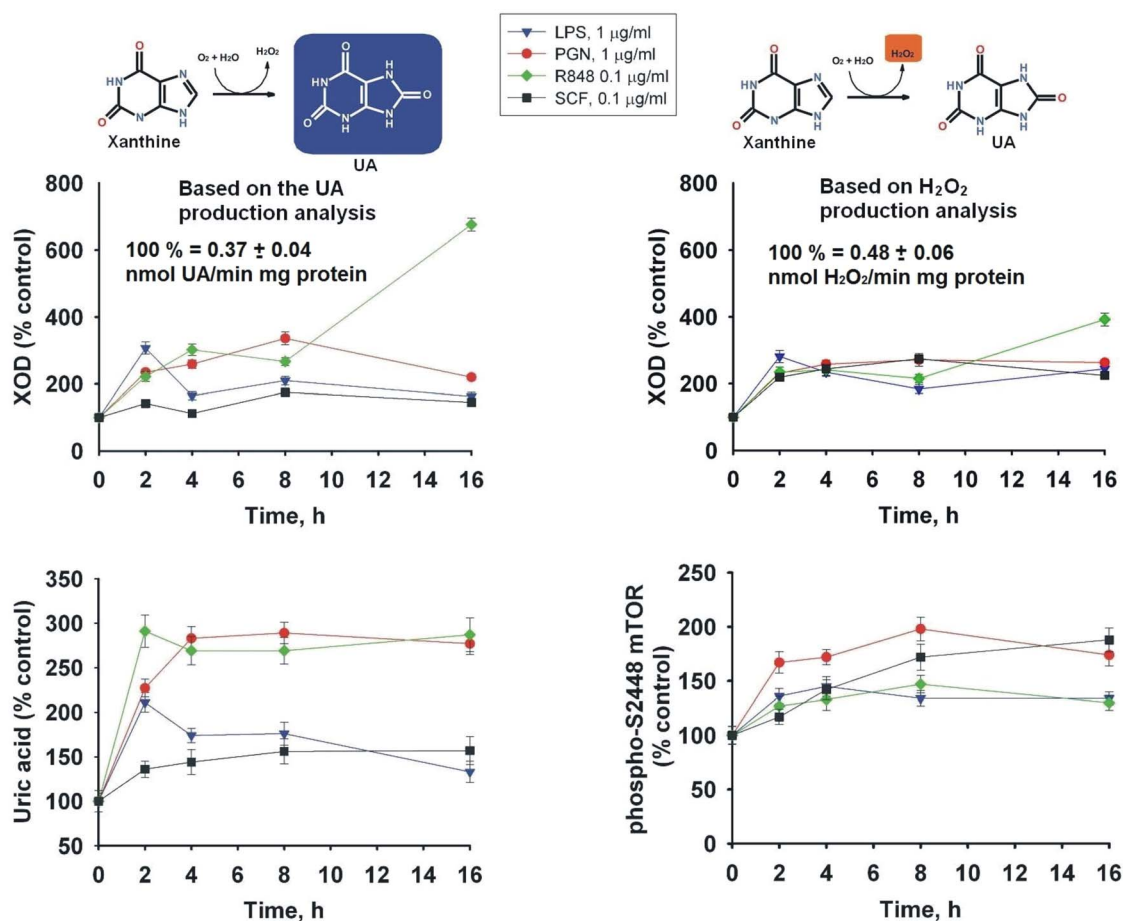


Figure 2 | LPS, PGN, R848 and SCF induce XOD activation and phosphorylation of S2448 mTOR in a time-dependent manner. THP-1 cells were exposed to 1 $\mu\text{g/ml}$ LPS, 1 $\mu\text{g/ml}$ PGN, 0.1 $\mu\text{g/ml}$ R848 as well as 0.1 $\mu\text{g/ml}$ SCF for different periods of time. XOD activity, intracellular UA levels and S2448 mTOR phosphorylation were analysed as described in Materials and Methods. Results are shown as mean values \pm S.D. of at least three independent experiments ($n=3-5$).

suggesting the presence of more AP-1 responsive elements than hypoxia (HIF-1) responsive elements¹.

We next assessed whether mTOR kinase, which acts as a key regulator of translation during myeloid cell responses, could also influence XOD activity, especially under conditions when HIF-1 is active. Our previous observations demonstrated that downregulation of mTOR during myeloid cell biological reactions reduces HIF-1 activity^{10,16}. From the experiments above, and previous observations, we know that HIF-1 is involved in XOD activation. We therefore pre-treated the cells with 30 μM LY294002 (phosphatidylinositol-3 kinase, PI-3K, inhibitor) together with or without 50 μM CoCl_2 (a classic mTOR-independent HIF-1 activator)^{8,16} for 1 h followed by 4 h of exposure to 1 $\mu\text{g/ml}$ PGN. We used LY294002 and not rapamycin since we found that rapamycin directly activates purified bovine XOD with the $K_a = 2.36$ μM (Supplementary figure 6A and Supplementary table 1). PI-3K is the upstream kinase for mTOR which is crucial for mTOR activation during TLR and SCF/Kit-mediated responses of myeloid cells. In the described experiment we measured XOD activity, phospho-S2448 mTOR and HIF-1 DNA-binding activity. We found that downregulation of mTOR is associated with PGN-induced XOD activation regardless of HIF-1 status (Figure 3C).

The role of the p38 MAP kinase pathway in XOD activation during human myeloid cell activation. Previous studies suggested a possible role for p38 MAP kinase in XOD activation^{1,17} and we next set out to provide definitive evidence to support this notion. First of all, we exposed THP-1 cells to 1 $\mu\text{g/ml}$ LPS, 1 $\mu\text{g/ml}$ PGN, 0.1 $\mu\text{g/ml}$ R848

as well as 0.1 $\mu\text{g/ml}$ SCF for 4 h followed by Western blot analysis of p38 MAP kinase phosphorylation and total protein amount of the kinase. We found that all the stimuli, especially LPS and SCF, induced p38 MAP kinase phosphorylation, however, R848 was the weakest inducer (Figure 4A), which is consistent with our previous observations on the functional role of p38 MAP kinase in different types of TLR-mediated responses^{8,14}. We then investigated the role of p38 MAP kinase in LPS (ligand of the plasma membrane-associated receptor) and R848 (ligand of the endosomal receptor) mediated responses. For this purpose, THP-1 cells were pre-treated for 1 h with 1 μM SB203580 (a p38 MAP kinase inhibitor) followed by a 4 or 24 h exposure to 1 $\mu\text{g/ml}$ LPS or 0.1 $\mu\text{g/ml}$ R848. We found that p38 MAP kinase was involved in LPS-induced XOD activation but not involved in the R848-induced response (Figure 4 B and C), which is in line with our previous observations for other signalling processes^{8,14}.

Since it has been proposed that p38 MAP kinase might be directly phosphorylating XOD we investigated whether additional phosphorylation of this enzyme is crucial for the investigated myeloid cell responses. THP-1 cells were exposed for 4 h to 1 $\mu\text{g/ml}$ LPS, 1 $\mu\text{g/ml}$ PGN, 0.1 $\mu\text{g/ml}$ R848 or 0.1 $\mu\text{g/ml}$ SCF followed by cell lysis and a 1 h exposure to alkaline phosphatase. XOD activity was then analysed. Treatment with alkaline phosphatase did not affect ligand-induced XOD activation (Figure 5A). We then analysed whether phosphate groups are crucial for the catalytic activity of purified bovine XOD. We exposed purified bovine XOD to alkaline phosphatase and found that this treatment did not change XOD catalytic activity (Figure 5B).

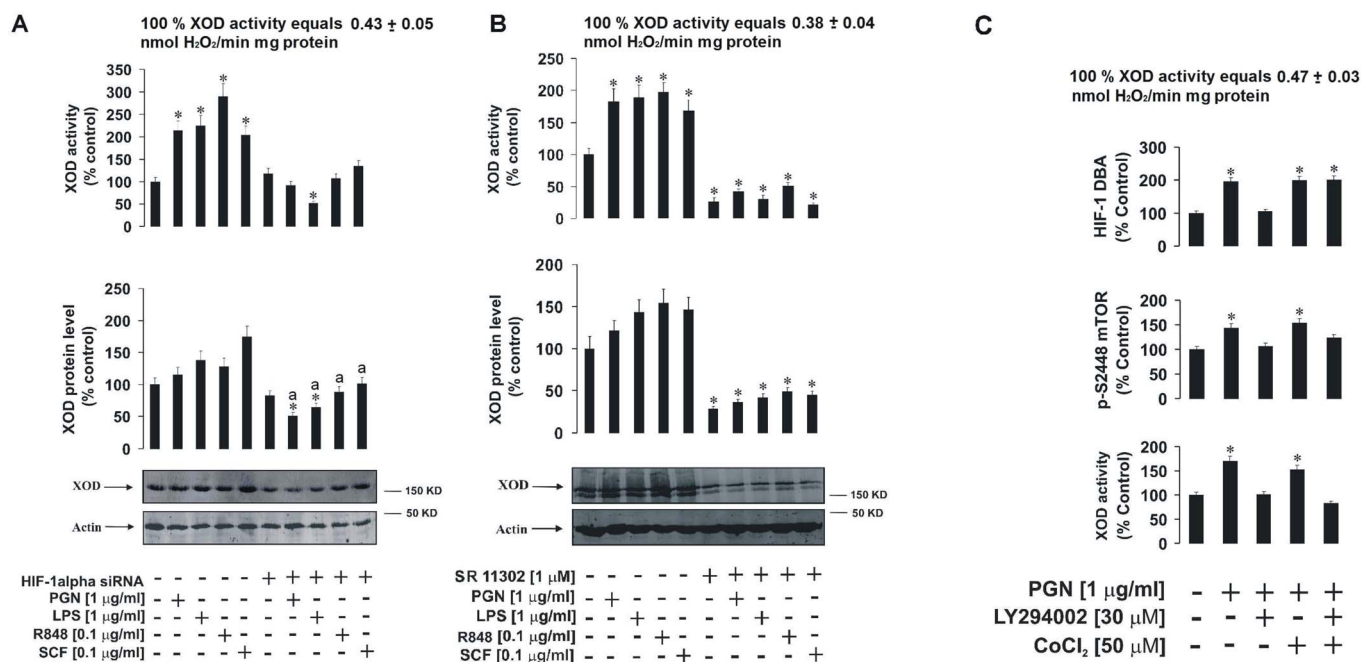


Figure 3 | HIF-1, AP-1 and mTOR play a role in maintaining XOD activity during the biological responses of THP-1 myeloid cells. (A) Normal and HIF-1 α knockdown THP-1 cells were exposed to 1 μ g/ml LPS, 1 μ g/ml PGN, 0.1 μ g/ml R848 as well as 0.1 μ g/ml SCF for 4 h followed by Western blot analysis of XOD protein levels and activity assay. (B) THP-1 cells were exposed to 1 μ g/ml LPS, 1 μ g/ml PGN, 0.1 μ g/ml R848 as well as 0.1 μ g/ml SCF for 4 h with or without 1 h pre-treatment with 1 μ M SR11302 (AP-1 inhibitor). Approximately 90 μ g protein was loaded onto the gel (in order to be able to visualise XOD in all samples, since the AP-1 inhibitor causes a strong downregulation in XOD protein levels). (C) THP-1 cells were exposed for 4 h to 1 μ g/ml PGN (a highly efficacious mTOR activator) with or without 1 h pre-treatment with 10 μ M Rapamycin (mTOR inhibitor). In some cases, 50 μ M cobalt chloride was added to maintain high HIF-1 activity. XOD activity, phospho-S2448 mTOR and HIF-1 DNA-binding activity (DBA) were measured as described in Materials and Methods. Western blot data show one representative experiment of three that gave similar results and were quantitatively analysed. Cropped blots are used. Full-length blots are presented in Supplementary Figures 2 and 3. Other quantitative data are shown as mean values \pm S.D. of at least three independent experiments; (n=3–4) * – p < 0.01 vs. control; a – p < 0.01 vs. corresponding treatment.

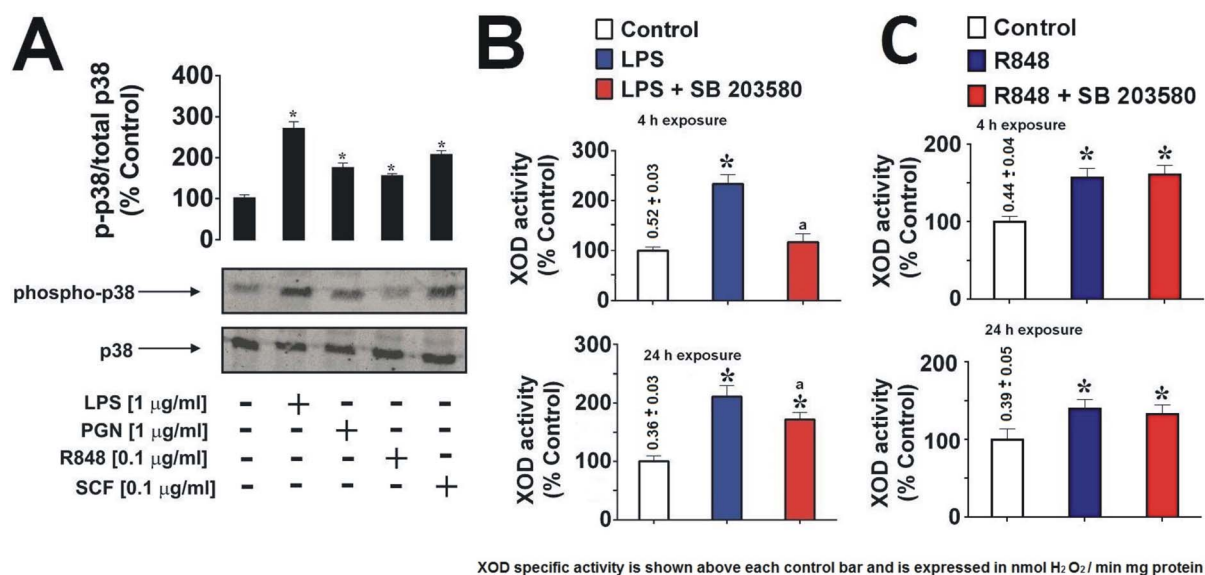


Figure 4 | The role of p38 MAP kinase in XOD activation in THP-1 myeloid cells. (A) THP-1 cells were exposed to 1 μ g/ml LPS, 1 μ g/ml PGN, 0.1 μ g/ml R848 as well as 0.1 μ g/ml SCF for 4 h followed by Western blot analysis of phospho-p38 MAP kinase *versus* total p38 MAP kinase. Cropped blots are used. Full-length blots are presented in Supplementary Figure 5. (B) THP-1 cells were exposed for 4 or 24 h to 1 μ g/ml LPS ((B) the strongest p38 MAP kinase inducer) or 0.1 μ g/ml R848 ((C) the weakest p38 MAP kinase activator) with or without 1 h pre-treatment with 1 μ M SB203580 (p38 MAP kinase inhibitor). XOD activity was analysed as described in Materials and Methods. Results are shown as mean values \pm S.D. of at least three independent experiments; (n=3–6) * – p < 0.01 vs. control.

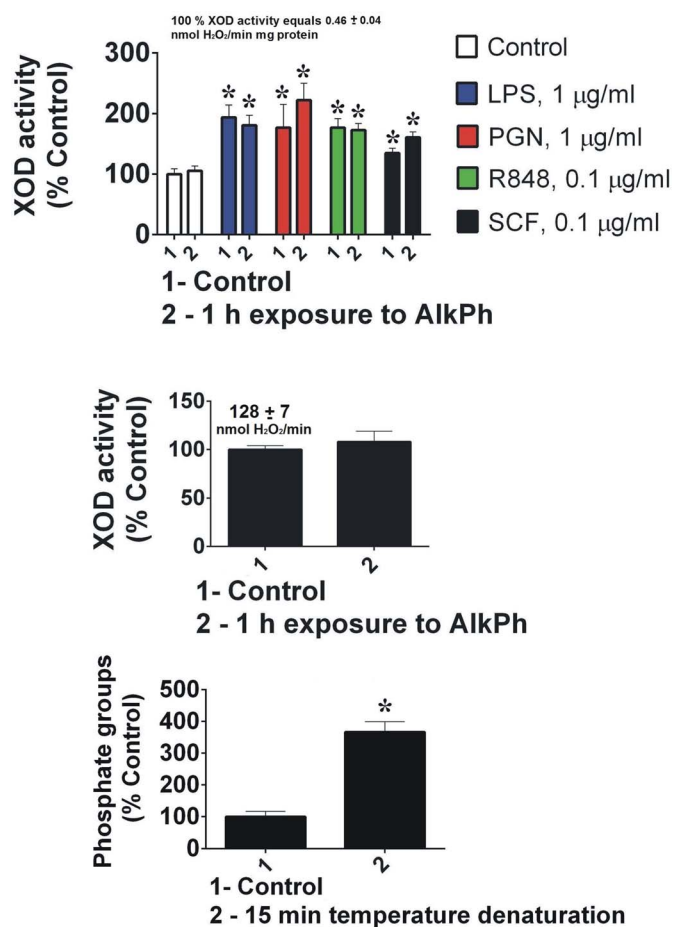


Figure 5 | XOD contains phosphate groups which are buried within its structure. (A) THP-1 cells were exposed to 1 $\mu\text{g/ml}$ LPS, 1 $\mu\text{g/ml}$ PGN, 0.1 $\mu\text{g/ml}$ R848 as well as 0.1 $\mu\text{g/ml}$ SCF for 4 h followed by XOD activity measurement with or without 1 h pre-exposure to alkaline phosphatase. (B) Activity of purified bovine XOD was measured with or without 1 h pre-exposure to alkaline phosphatase. (C) Phosphate groups were detected in purified bovine XOD before and after 15 min temperature (95°C) denaturation. Results are shown as mean values \pm S.D. of at least three independent experiments; (n=3–6) * – $p < 0.01$ vs. control.

Finally, we investigated whether XOD contains phosphate groups at all. For this purpose we quantified phosphate groups in purified bovine XOD. We analysed both unmodified protein as well as following 15 min of temperature denaturation (boiling the preparation at 95°C). We found that the amount of detectable phosphate groups was significantly higher in the denatured protein suggesting that the phosphate groups are buried within the XOD structure (Figure 5C).

XOD activity is essential for S2448 mTOR phosphorylation during the biological responses of human myeloid cells. We investigated whether XOD, as a crucial purine catabolising enzyme, plays a role in myeloid cell signalling during TLR-mediated and SCF/Kit-induced responses of human hematopoietic cells of myeloid lineage. We pre-treated THP-1 cells with 250 $\mu\text{g/ml}$ allopurinol (XOD isosteric inhibitor, $K_i = 1.82$ mM, see Supplementary figure 6A, Supplementary table 1) followed by exposure to 1 $\mu\text{g/ml}$ LPS, 1 $\mu\text{g/ml}$ PGN, 0.1 $\mu\text{g/ml}$ R848 or 0.1 $\mu\text{g/ml}$ SCF. We then measured XOD activity and intracellular UA content. Activity of PI-3K and the intracellular levels of phospho-S2448 mTOR were also analysed. We found that XOD activity and UA production were induced by all four stimuli. This was in line with a significant increase in PI-3K activity and S2448 mTOR phosphorylation (Figure 6). Pre-treatment with allopurinol

attenuated XOD activation/UA production. The amount of phospho-S2448 mTOR but not PI-3K activity was decreased by allopurinol (Figure 6). It is known that XOD inhibition leads to intracellular hypoxanthine accumulation³. Hypoxanthine could then be re-cycled and converted into inosine monophosphate (IMP) and further into AMP, which allosterically activates AMP kinase (AMPK)^{7,18}. AMPK is a physiological inhibitor of mTOR which leads to its phosphorylation at T2446, thus preventing phosphorylation of the S2448 and therefore mTOR activation. To investigate whether this is indeed the case, we performed treatments described above and compared the phosphorylation of mTOR at S2448 and T2446. We found that allopurinol decreased ligand-induced S2448 mTOR phosphorylation while significantly increasing T2446 phosphorylation (Supplementary figure 7A). To investigate whether specific XOD inhibition increases intracellular AMP levels we pre-treated the cells for 1 h with 100 $\mu\text{g/ml}$ sodium tungstate (Na_2WO_4). Tungsten replaces Mo in the XOD structure, thus attenuating its activity ($K_i = 1.09$ mM, see Supplementary figure 6B and Supplementary table 1). We used sodium tungstate as an alternative inhibitor, also because we were interested in measuring intracellular AMP levels (allopurinol is a hypoxanthine isomer which could possibly affect successful AMP measurement). Na_2WO_4 attenuated ligand-induced XOD activation and significantly increased its T2446 phosphorylation as well as intracellular AMP levels (Supplementary figure 7B).

To check whether specific induction of XOD activity leads to any changes in intracellular AMP levels and mTOR phosphorylation we exposed THP-1 cells for 24 h to 100 $\mu\text{g/ml}$ ammonium molybdate ($(\text{NH}_4)_6\text{Mo}_7\text{O}_{24}$), which specifically induces post-translational activation of XOD (since XOD is a molybden-containing enzyme)¹⁹. We found that XOD activity was significantly increased (Supplementary figure 8). This was in line with a decrease in intracellular AMP levels. However, no changes in mTOR phosphorylation on S2448 or T2446 were observed (Supplementary figure 8).

PGN upregulates XOD activity, UA production, and the PI-3K/mTOR pathway in mouse blood and liver *in vivo*. We finally asked whether the responses investigated in our *in vitro* studies regarding TLR ligand-induced activation of XOD and the essential role of the PI-3K/mTOR pathway actually take place *in vivo*. Six-week-old CD1 male mice (25 \pm 5 g) were systemically injected with 1 mg/kg PGN and sampled 4 h post-injection as described in the Materials and Methods. We found that PGN induced XOD activity in blood cells and liver. This was in line with increased UA levels in blood plasma and liver (Figure 7). Moreover, the activity of PI-3K and S2448 mTOR phosphorylation levels in blood cells and liver homogenates of PGN-injected mice were significantly upregulated compared to the control groups (Figure 7). These results suggest that the activation of both XOD and PI-3K/mTOR pathway are induced by TLR ligands *in vivo*. Furthermore, they are induced not only in blood cells but also in the liver – where XOD activity is naturally the highest.

Discussion

Our investigations clearly confirm the hypothesis of involvement of XOD in controlling signalling networks associated with functioning of human myeloid hematopoietic cells. Previous reports suggested an upregulation of this purine catabolising enzyme during TLR-mediated and growth factor/cytokine-induced responses of human myeloid cells^{1,7,8,20}. Our studies confirmed that XOD activity as well as UA production is induced in human myeloid leukaemia cells exposed to ligands of plasma membrane-associated TLRs 2 and 4, endosomal TLRs 7/8 as well as the SCF/Kit receptor (Figure 2).

Our study showed that the upregulation of XOD was taking place more on the level of catalytic activity rather than increasing XOD protein levels, as shown by our Western blot analysis (Figure 3 A and B). It was, however, found that HIF-1 and AP-1 transcription factors

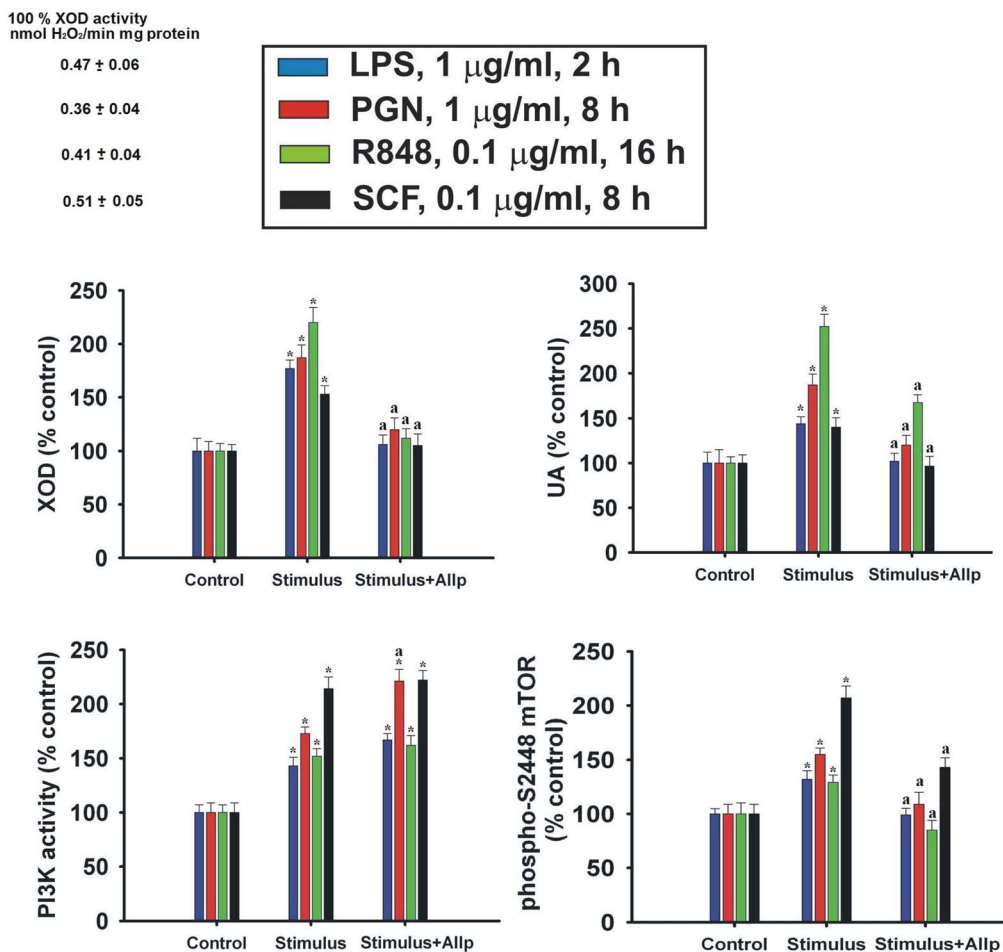


Figure 6 | XOD plays a crucial role in S2448 mTOR phosphorylation during the biological responses of THP-1 human myeloid cells. THP-1 cells were exposed to 1 µg/ml LPS, 1 µg/ml PGN, 0.1 µg/ml R848 as well as 0.1 µg/ml SCF for indicated periods of time with or without 1 h pre-treatment with 250 µg/ml allopurinol. XOD activity, intracellular UA levels, PI-3K activity were measured as outlined in Materials and Methods. Results are shown as mean values ± S.D. of at least three independent experiments; (n=3–5) * – p < 0.01 vs. control.

are required to maintain XOD levels in myeloid leukaemia cells, since directed attenuation of HIF-1 or AP-1 activity significantly reduced XOD protein levels as well as its activity in human myeloid cells regardless of the stimulus employed (Figure 3 A and B). Importantly, translational control operated by the mTOR complex appeared to be directly involved in ligand-induced XOD activation in human myeloid leukaemia cells (Figure 3C). These results demonstrate that AP-1 and HIF-1 are clearly involved in ligand-induced XOD upregulation. Recent evidence suggested that LPS, PGN, R848 and SCF induce activation of mTOR, which appears crucial for upregulation of the HIF-1 transcriptional activity¹⁶. However, in the present study we demonstrate that mTOR influences XOD activation independently of HIF-1. The activity of HIF-1 was kept at a high level with the help of cobalt chloride. But this could not restore a rapamycin-dependent decrease in ligand-induced XOD upregulation in human myeloid leukaemia cells, despite the fact that rapamycin could directly activate XOD (Supplementary figure 6, Supplementary table 1).

Further studies demonstrated the importance of p38 MAP kinase in XOD activation *via* plasma membrane-associated TLR4 but not endosomal TLRs 7/8 (Figure 4). This is in line with our recent observations where p38 MAP kinase was critically involved in stress adaptation pathways in myeloid cells during LPS/TLR4-induced responses but not R848/TLRs7/8-dependent events^{8,14}. It is important to mention that R848 appeared the weakest p38 MAP kinase activator compared to other stimuli (PGN, LPS and SCF) used. p38 MAP

kinase is more likely to be involved indirectly (for example through activation of the AP-1 transcription complex)²¹ because phosphate groups appeared to be hidden in the XOD structure and could not be accessed by alkaline phosphatase (Figure 5).

Further studies demonstrated that XOD activation is crucial for translational control. Specific inhibition of XOD by allopurinol significantly reduced ligand-dependent activation of S2448 mTOR phosphorylation but not PI-3K (Figure 6). This effect most likely took place due to provoking the recycling of hypoxanthine due to the inability of XOD to convert it further. Re-use of hypoxanthine includes its two-stage conversion into AMP (the allosteric activator of AMP kinase), which inhibits mTOR through phosphorylation of T2446. Inhibition of XOD led to an increase in intracellular AMP levels and phospho-T2446 mTOR which reduced the amounts of the phospho-S2448 mTOR (Supplementary figure 7). However, the changes in S2448 phosphorylation of mTOR do not merely result from XOD activation since specific molybden-dependent induction of XOD activity has no effect on mTOR phosphorylation in the absence of TLR or Kit ligands (Supplementary figure 8). Proposed possible mechanisms underlying XOD activation in human myeloid cells during their biological responses are summarised in the Supplementary figure 9.

Activation of both XOD and the PI-3K/mTOR pathway was observed in blood cells and liver of mice *in vivo* too (Figure 7), following injection of mice with 1 mg/kg TLR2 ligand PGN. These observations provide an *in vivo* confirmation of the results obtained

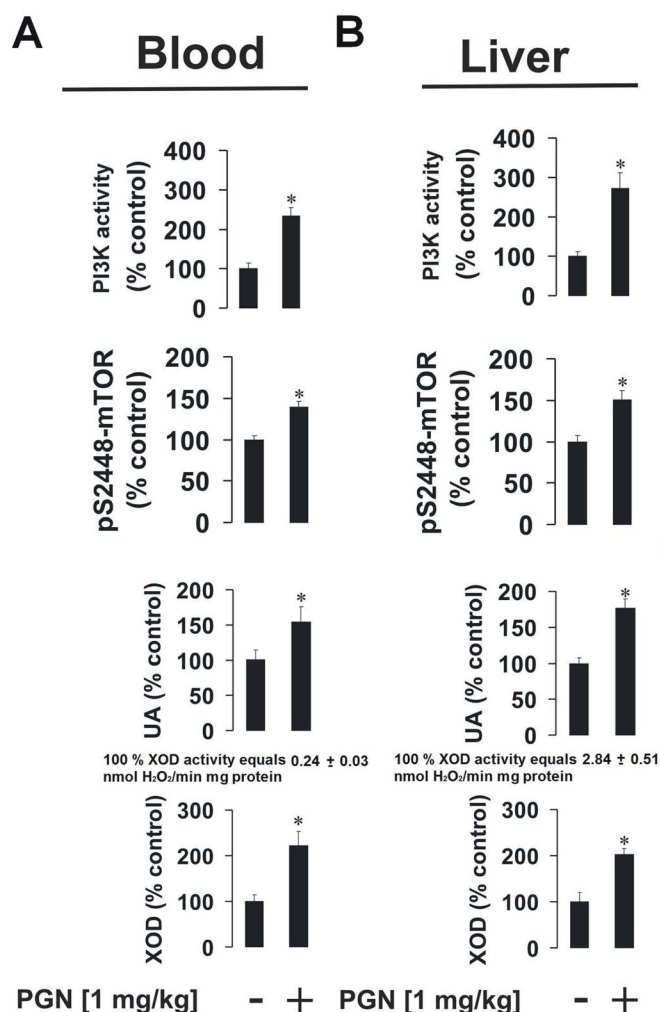


Figure 7 | PGN activates XOD and PI-3K/mTOR pathway *in vivo*.

Twenty (four groups of five animals) six week old male CD1 mice were used as outlined in Materials and Methods. Blood was collected and the liver was isolated and homogenised. XOD activity, phospho-S2448 mTOR, and PI-3K activity were measured in blood cells and liver. UA levels were detected in the blood plasma (A) and liver (B). Quantitative data are mean values \pm S.D. (n=5); *p < 0.05 vs. control.

in vitro, at least to a certain extent. Unlike humans, however, mice are capable of degrading UA into allantoin, UA levels in these animals are quite high so that this compound can still act as a “danger signal”^{8,22,23}.

Taken together, our results demonstrate for the first time that XOD is not just activated in human myeloid cells by pro-inflammatory stimuli/SCF but also plays an important role in maintaining mTOR-dependent translational control during biological responses of these cells. These findings open the new route in myeloid cell, inflammation and leukaemia research, since XOD can now be considered for investigation as a potential target for curing autoimmune disease and to relief undesired inflammatory reactions.

Methods

Materials, cells (THP-1, MCF-7, LAD2²⁴ and primary human basophils) and animals (mice) used in the work are described in the Supplementary information.

Animal experiments were performed following approval by the Institutional Animal Committee and handled in accordance with the Animals (Scientific Procedures) Act 1986 and Helsinki Declaration.

Transfer of HIF-1 α siRNA into THP-1 cells. We employed a HIF-1 α -specific siRNA target sequence (ugu gag uuc gca ucu uga u dtdt) which was localised at position 146 bases downstream of the HIF-1 α start codon⁶⁷. Transfection into THP-1 cells was

performed using DOTAP reagent according to the manufacturer’s protocol. Successful silencing of HIF-1 α was controlled by quantitative real-time PCR (qRT-PCR). Total RNA was isolated using a GenEluteTM mammalian total RNA miniprep kit, followed by a HIF-1 α mRNA reverse transcriptase–polymerase chain reaction (RT-PCR) in accordance with the manufacturer’s protocols after which qRT-PCR was performed. Primer selection was as follows: HIF-1 α , 5’-CTCAAAGTCGGAC-AGCCTCA-3’, 5’-CCCTGCAGTAGGTTCTGCT-3’ actin, 5’-TGACGGGT-CAC-CCACACTGTGCCATCTA-3’, 5’-CTAGAAGCATTTCGGTTCGACGA-TGGAGG-3’⁷. Reactions were performed using a LightCycler[®] 480 real-time PCR system and respective SYBR Green I Master kit (Roche, Burgess Hill, UK). Analysis was carried out according to the manufacturer’s protocol. Values representing HIF-1 α mRNA levels were normalised against those of actin⁷. Corresponding random siRNA (uac acc guu agc aga cac c dtdt) had no effect on the studied processes⁷.

Detection of XOD activity and UA levels. XOD activity was detected spectrophotometrically using two methods^{4,7}. One was based on the ability of XOD to convert xanthine into UA, which was quantified spectrophotometrically (see Figure 2 for the reaction). 50 μ l of borate buffer (0.2 M boric acid mixed with 0.05 M sodium tetraborate), pH 8.2 (XOD pH optimum) was mixed with 50 μ l of 2 mM xanthine (xanthine was initially dissolved in a minimal volume of 0.01 M NaOH and brought to the desired volume and the pH adjusted to 8.2). 50 μ l of cell lysate (or tissue homogenate) was added and samples were then incubated for 60–120 min at 40°C (optimum temperature for XOD activity). Proteins were then precipitated using 0.35 M H₂SO₄ and 0.3 M sodium tungstate solution. This was followed by detection of UA using a phosphotungstate assay: alkaline conditions were generated using a 0.95 M sodium carbonate solution. Phosphotungstate reagent was prepared by mixing 40 g of sodium tungstate and 300 ml of bidistilled deionised water. 32 ml of concentrated phosphoric acid (15.2 M) was added and the mixture was then boiled for 2 h before cooling to room temperature. The volume was adjusted to 1 l and 32 g of lithium sulphate was dissolved in the reagent. The phosphotungstate reagent was then stored in a dark bottle at 4°C. UA reduces phosphotungstate reagent forming a steady blue colour (the absorbance was analysed at 650 nm). The amount of UA was calculated using a calibration curve obtained from the analysis of standard UA solutions (concentration range – 6.25–1000 μ M). Control samples (blank) did not contain xanthine (since xanthine does not react with phosphotungstate reagent at all but cell lysate/tissue homogenate could contain traces of uric acid). XOD activity was expressed in nmol UA produced per 1 min per mg protein. Controls were normalised and expressed as 100%. XOD activities in other samples were expressed as % control.

The other assay was based on the detection of hydrogen peroxide produced by XOD after converting xanthine into UA (see Figure 2 for the reaction) as described previously^{4,25}. 60 μ l of 0.1 M Tris containing 40 mg/l horseradish peroxidase (HRP) buffer (pH 7.5 – this pH is perfectly suitable for both XOD and HRP as well as for quenching reactions) were mixed with 20 μ l 2 mM xanthine (see above) and 10 μ l of ortho-phenylenediamine water solution. Reactions were started by adding 20 μ l of sample (the amount could be increased to 50 μ l in the case of weak activity). Control samples (blank) did not contain xanthine. Samples were incubated for 30 min at 40°C followed by termination of the reaction with 100 μ l of 1.88 M H₂SO₄ solution. H₂O₂ standards were analysed to calculate XOD activity (concentrations – 0.1–100 nmol/ml). The absorbance was measured at 492 nm. XOD activity was expressed in nmol H₂O₂ produced per 1 min per mg protein. Controls were normalised as 100%. XOD activities in other samples were expressed as % control.

UA levels were analysed by colorimetric assay using phosphotungstate reagent as described above²⁴.

Western blot analysis. Intracellular XOD protein as well as phospho-p38/total p38 MAP kinase levels were determined by Western blot analysis and compared to β -actin to assess equal loading, as we previously reported¹⁹. When analysing relative XOD expression in different cell types and p38 MAP kinase levels we loaded 50 μ g protein per well in SDS PAGE. When analysing XOD protein levels in THP-1 myeloid cells, 50–100 μ g protein per well was loaded. Li-Cor (Lincoln, Nebraska USA) secondary antibodies (conjugated with fluorescent dyes) were used according to the manufacturer’s protocol in order to visualise the proteins of interest in a Li-Cor Odyssey imaging system. Using Odyssey software, Western blot data were subjected to quantitative analysis and values were normalised against respective β -actin bands.

Detection of phospho-S2448 and phospho-T2446 mTOR in cell lysates by ELISA. ELISA was employed to analyse S2448 or T2446 phosphorylation of mTOR as we previously described⁷. Briefly, plates coated with mouse anti-mTOR antibody and blocked with 1% BSA were incubated with cell lysates at room temperature for at least 2 h with constant agitation. Plates were then washed with TBST (10 mM Tris-HCl, pH 8.0, 150 mM NaCl, 0.05% Tween-20) buffer and anti-phospho-S2448 (or anti-phospho-T2446) mTOR antibody was added followed by a 2 h incubation at room temperature (with agitation). Plate were then washed 5 times with TBST buffer and incubated with 1 : 1000 HRP-labelled goat anti-rabbit IgG in TBST buffer for at least 2 h. After extensive washing with TBST, bound secondary antibodies were detected by the peroxidase reaction (ortho-phenylenediamine/H₂O₂) as described.

Determination of HIF-1 DNA-binding activity. HIF-1 DNA-binding activity (HIF-1 DBA) was measured using the method we described recently⁷. Briefly, 96-well MaxisorpTM microtitre plates were coated with streptavidin and blocked with BSA. 2 pmol/well biotinylated 2HRE-containing oligonucleotide were immobilised by 1 h incubation of the plates at room temperature. Plates were then washed 5 times with



TBST buffer followed by 1 h incubation with 20 μ l/well of cell lysate at room temperature. After washing the plates 5 times with TBST buffer mouse anti-HIF-1 α antibody (1 : 1000 in TBS plus 2% BSA) was added and plates were incubated for 1 h before a further washing cycle. 1 : 1000 HRP-labelled rabbit anti-mouse IgG in TBST buffer was then added to the wells and, after extensive washing with TBST, bound secondary antibodies were detected by the peroxidase reaction (orthophenylenediamine/H₂O₂).

Detection of PI-3K activity, AMP levels and phosphate groups. PI-3K activity was detected based on the previously described approach²⁶. Briefly, cell lysates were each incubated with 30 μ l 0.1 mg/ml substrate (PI-4,5-diphosphate – the emulsion was prepared using bidistilled water; sonication for 1 hour in a water bath sonicator is recommended) in kinase assay buffer. The latter was prepared from 20 mM Tris (pH 7.5), 100 mM NaCl, 0.5 mM EDTA, 8 mM MgCl₂ and 40 μ M ATP in a total volume of 100 μ l at 37°C with constant agitation. Reactions were stopped by adding 1 ml of mixture hexane/isopropanol (13 : 7, v : v) and 0.2 ml of a mixture of 2 M KCl/HCl_{conc} (8 : 0.25, v : v). Samples were vortexed and organic phases were washed with HCl (0.5 ml; 0.1 M). This was followed by detection of phosphate groups using molybdenum reagent^{25,27} containing 2 parts of 25 mM (NH₄)₆Mo₇O₂₄, 5 parts of H₂SO₄ (140 ml of H₂SO_{4 conc} was diluted to 900 ml with bidistilled water), 2 parts of 0.3 M ascorbic acid and 1 part of 2 mM potassium antimonyl-tartrate^{25,26}. In case of very high or low absorbance, the product (PI-3,4,5-triphosphate) should be separated by thin-layer chromatography (TLC) using silica gel TLC plates (chromatographic mixture of 2 M acetic acid/isopropanol (1 : 2, v : v) has to be applied) and detected using molybdenum reagent. The values obtained in the control samples of each experiment per 1 mg protein were counted as 100% of the PI-3K activity. Other values were normalised and expressed as % control.

Intracellular AMP levels were detected based on the use of a commercial Promega AMP luminometric assay kit according to the manufacturer's protocols.

Phosphate groups in the purified protein were detected using molybdenum reagent as described above.

Statistical analysis. Each experiment was performed at least three times and statistical analysis was conducted using a sample distribution analysis followed by a two-tailed Student's t test. Statistical probabilities (p) were expressed as *, where p < 0.01.

- Berry, C. E. & Hare, J. M. Xanthine oxidoreductase and cardiovascular disease: molecular mechanisms and pathophysiological implications. *J. Physiol.* **555**, 589–606 (2004).
- Hille, R. & Nishino, T. Flavoprotein structure and mechanism. Xanthine oxidase and xanthine dehydrogenase. *FASEB. J.* **9**, 995–1003 (1995).
- George, J. & Struthers, A. D. (2009). Role of urate, xanthine oxidase and the effects of allopurinol in vascular oxidative stress. *Vasc. Health Risk Manag.* **5**, 265–272 (2009).
- Sumbayev, V. V. In vitro effects of corticosteroids, DDT, and 4, 9-dichlorodibenzodioxin on rat liver xanthine oxidase activity. Interactions between xanthine oxidase and cytochrome P450 in rat liver in vivo. *Biochemistry (Mosc.)* **65**, 972–975 (2000).
- Gibbins, S. *et al.* Xanthine oxidoreductase promotes the inflammatory state of mononuclear phagocytes through effects on chemokine expression, peroxisome proliferator-activated receptor- γ sumoylation, and HIF-1 α . *J. Biol. Chem.* **286**, 961–975 (2011).
- Nicholas, S. A., Bubnov, V. V., Yasinska, I. M. & Sumbayev, V. V. Involvement of xanthine oxidase and hypoxia-inducible factor 1 in Toll-like receptor 7/8-mediated activation of caspase 1 and interleukin-1 β . *Cell Mol. Life Sci.* **68**, 151–158 (2011).
- Yasinska, I. M., Gibbs, B. F., Lall, G. S. & Sumbayev, V. V. The HIF-1 transcription complex is essential for translational control of myeloid hematopoietic cell function by maintaining mTOR phosphorylation. *Cell. Mol. Life Sci.* **71**, 699–710 (2014).
- Nicholas, S. A. & Sumbayev, V. V. The involvement of hypoxia-inducible factor 1 α in Toll-like receptor 7/8-mediated inflammatory response. *Cell Res.* **19**, 973–983 (2009).
- Sumbayev, V. V., Nicholas, S. A., Streatfield, C. L. & Gibbs, B. F. Involvement of hypoxia-inducible factor-1 HIF(1 α) in IgE-mediated primary human basophil responses. *Eur. J. Immunol.* **39**, 3511–3519 (2009).
- Gibbs, B. F., Yasinska, I. M., Oniku, A. E. & Sumbayev, V. V. Effects of stem cell factor on hypoxia-inducible factor 1 α accumulation in human acute myeloid leukaemia and LAD2 mast cells. *PLoS One* **6**, e22502 (2011).
- Xu, P., Huecksteadt, T. P. & Hoidal, J. R. Molecular cloning and characterization of the human xanthine dehydrogenase gene (XDH). *Genomics* **34**, 173–180 (1996).
- Hoidal, J. R., Xu, P., Huecksteadt, T., Sanders, K. A. & Pfeffer, K. Transcriptional regulation of human xanthine dehydrogenase/xanthine oxidase. *Biochem. Soc. Trans.* **25**, 796–799 (1997).
- Xu, X. *et al.* Xanthine oxidase inhibition with febuxostat attenuates systolic overload-induced left ventricular hypertrophy and dysfunction in mice. *J. Card. Fail.* **14**, 746–753 (2008).
- Sumbayev, V. V. LPS-induced Toll-like receptor 4 signalling triggers cross-talk of apoptosis signal-regulating kinase 1 (ASK1) and HIF-1 α protein. *FEBS Lett.* **582**, 319–326 (2008).
- Hellsten-Westling, Y. Immunohistochemical localization of xanthine oxidase in human cardiac and skeletal muscle. *Histochemistry* **100**, 215–222 (1993).
- Gibbs, B. F., Yasinska, I. M., Pchejetski, D., Wyszynski, R. W. & Sumbayev, V. V. Differential control of hypoxia-inducible factor 1 activity during pro-inflammatory reactions of human hematopoietic cells of myeloid lineage. *Int. J. Biochem. Cell Biol.* **44**, 1739–1749 (2012).
- Kayyali, U. S., Donaldson, C., Huang, H., Abdelnour, R. & Hassoun, P. M. Phosphorylation of xanthine dehydrogenase/oxidase in hypoxia. *J. Biol. Chem.* **276**, 14359–14365 (2001).
- Gwinn, D. M. *et al.* AMPK phosphorylation of raptor mediates a metabolic checkpoint. *Mol. Cell* **30**, 214–226 (2008).
- Sumbayev, V. V., Karpova, O. V. & Studinskaia, T. B. Activity of nitric oxide synthase, poly-(ADP-ribose)-polymerase, protein kinase C, protein kinase ASK 1 and internucleosome fragmentation of DNA in HER-2 cells during molybdenum-induction of xanthine oxidase. *Ukr. Biokhim. Zh.* **73**, 119–122 (2001).
- Nomura, J. *et al.* Febuxostat, an inhibitor of xanthine oxidase, suppresses lipopolysaccharide-induced MCP-1 production via MAPK phosphatase-1-mediated inactivation of JNK. *PLoS One* **8**, e75527 (2013).
- Sumbayev, V. V. & Yasinska, I. M. Role of MAP kinase-dependent apoptotic pathway in innate immune responses and viral infection. *Scand. J. Immunol.* **63**, 391–400 (2006).
- Griffith, J. W., Sun, T., McIntosh, M. T. & Bucala, R. Pure Hemozoin is inflammatory in vivo and activates the NALP3 inflammasome via release of uric acid. *J. Immunol.* **183**, 5208–5220 (2009).
- Mulla, M. J. *et al.* A role for uric acid and the Nalp3 inflammasome in antiphospholipid antibody-induced IL-1 β production by human first trimester trophoblast. *PLoS One* **8**, e65237 (2013).
- Kirshenbaum, A. S. *et al.* Characterization of novel stem cell factor responsive human mast cell lines LAD 1 and 2 established from a patient with mast cell sarcoma/leukemia; activation following aggregation of Fc ϵ silonRI or Fc γ RI. *Leuk. Res.* **27**, 677–682 (2003).
- Dawson, R. M. C., Elliot, D. L., Elliot, W. H. & Jones, K. M. *Data for biochemical research* (Clarendon Press, Oxford, 1986).
- Kirsch, C., Wetzker, R. & Klinger, R. Anionic phospholipids are involved in membrane targeting of PI 3-kinase gamma. *Biochem. Biophys. Res. Commun.* **282**, 691–696 (2001).
- Schneider, R. & Daum, G. Analysis of Yeast Lipids. In: *Methods Mol. Biol., Yeast Protocols: second edition*, Humana Press Inc., Totowa, NJ, **313**, 75–84 (2006).

Author contributions

M.A. performed the experiments, analysed the data, prepared figures; G.S.L. performed animal experiments; H.S.L. and K.C. performed kinase assays; B.F.G. analysed the data, wrote the manuscript; V.V.S. designed all experiments, analysed the data, performed and supervised the experiments, wrote the manuscript, prepared figures. All authors reviewed the manuscript.

Additional information

Supplementary information accompanies this paper at <http://www.nature.com/scientificreports>

Competing financial interests: The authors declare no competing financial interests.

How to cite this article: Abooli, M. *et al.* Crucial involvement of xanthine oxidase in the intracellular signalling networks associated with human myeloid cell function. *Sci. Rep.* **4**, 6307; DOI:10.1038/srep06307 (2014).



This work is licensed under a Creative Commons Attribution-NonCommercial-NoDerivs 4.0 International License. The images or other third party material in this article are included in the article's Creative Commons license, unless indicated otherwise in the credit line; if the material is not included under the Creative Commons license, users will need to obtain permission from the license holder in order to reproduce the material. To view a copy of this license, visit <http://creativecommons.org/licenses/by-nc-nd/4.0/>